Journal of Ovonic Research Vol. 7, No. 4, July - August 2011, p. 73 - 82

VERIFICATION OF HUME-ROTHERY CONDITION OF PHASE STABILITY IN RAPIDLY SOLIDIFIED Sn-Zn BINARY ALLOYS

M. KAMAL, A. B. EL-BEDIWI, T. EL-ASHRAM[a*], M. E. DORGHAM
Metal Physics Lab., Physics Department, Faculty of Science, Mansoura University, Egypt.
[a]*Physics Department, Faculty of Science, Port Said University, Port Said, Egypt.*

A group of binary Sn-xZn alloys (x= 6, 7, 8, 9, 10 and 11wt.%) have been produced by a single copper roller melt-spinning technique. In this study the Hume-Rothery condition of phase stability has been verified. It is found that by increasing valence electron concentration VEC the diameter of Fermi sphere $2k_F$ increases which leads to the increase in the diameter of Brillouin zone. Also it has been confirmed that the correlation between Young's modulus and the axial ratio ***c/a*** of β-Sn unit cell, however there is a critical value of ***c/a*** about 0.54562 beyond which E decreases. It is found also that the volume and shape of the unit cell affect both electrical and mechanical properties.

(Received July 25, 2011, accepted August 12, 2011)

Keywords: Alloys, Rapid solidification, Valence electron concentration, Resistivity, Young's modulus, Fermi energy, Brillouin zone

1.Introduction

Hume- Rothery found that definite structures of compounds arise in certain ranges of the valence electron concentration [1]. These compounds are called Hume-Rothery compounds or electron compounds. Indeed, for these phases a band energy minimization occurs when the Fermi sphere touches a pseudo-Brillouin zone (prominent Brillouin zone), constructed by Bragg vectors K_B corresponding to intense peaks in the experimental diffraction pattern. When the Brillouin zone boundary touches the Fermi sphere, the structure corresponding to the zone will be stabilized. As a result, a pseudo-gap of density of states around the Fermi level will arise. This is the Hume-Rothery condition of phase stability i.e., $K_B = 2k_F$ where K_B is the diameter of the Brillouin zone and k_F is the radius of Fermi sphere.

Therefore the most important parameter affecting the structure, stability and properties of alloys is valence electron concentration (VEC). This quantity indicates the number of all valence electrons in the alloy per number of atoms. [2, 3] found that the axial ratio ***c/a*** of the β-Sn tetragonal unit cell increases by increasing VEC and decreases by decreasing VEC. This observation is confirmed recently by [4]. The increase in the axial ratio with decreasing VEC was explained qualitatively by [2, 5] on the basis of the interaction between Fermi surface and Brillouin zone. Also it is found by [6] that the most important factor for the formation of stable quasicrystals is the valence electron concentration. [4, 7] found a connection between Young's modulus and the axial ratio ***c/a*** of the tetragonal unit cell of β-Sn. They observed that Young's modulus increases by increasing the axial ratio and the resistivity decreases by increasing ***c/a***. This means that the dependence of both Young's modulus and resistivity on VEC.

Fermi parameters such as Fermi energy E_F, radius of Fermi sphere k_F Fermi velocity v_F, and the diameter of the Brillouin zone K_B can be calculated from the following equations;

$$E_F = \frac{\hbar^2}{2m}\left(\frac{3\pi^2 N}{V}\right)^{\frac{2}{3}},\quad k_F = \left(\frac{3\pi^2 N}{V}\right)^{\frac{1}{3}},\quad v_F = \frac{\hbar k_F}{m},\quad K_{Bhkl} = \frac{2\pi}{d_{hkl}}$$

*Corresponding author: tnelashram@gmail.com.

where N/V is the total number of electrons per unit volume in the alloy, m is the effective mass, $\hbar$ is the reduced Plank's constant and d_{hkl} is the interplanar distance.

The objective of the present work is to verify the Hume-Rothery condition of phase stability and to study the structure and properties of rapidly solidified Sn-Zn binary alloys using single roller melt-spinning technique. Rapid solidification has been used in the present work to prevent rejection of extra solute atoms and thus prevent precipitation, from a solid solution.

2. Experimental procedures

A group of binary Sn--xZn alloys (x= 6, 7, 8, 9, 10 and 11wt.%) have been produced by a single copper roller melt-spinning technique. Required quantities of the used metals were weighed out and melted in a porcelain crucible. After the alloys were molten, the melt was thoroughly agitated to effect homogenization. The casting was done in air at a melt temperature of 800 °C. The speed of the copper wheel was fixed at 2900 r.p.m. which corresponds to a linear speed of 30.4 $m.s^{-1}$. X-ray diffraction analysis is carried out with a Shimadzu x-ray diffractometer (DX-30), using Cu-K_α radiation with a Ni-filter (λ = 0.154056 nm). Differential thermal analysis (DTA) is carried out in a Shimadzu DT-50 with heating rate 10 K/min. The measurement of resistivity is carried out by the double bridge method [8]. Young's modulus was measured by the dynamical resonance method [9]. Vickers microhardness number (HV) is measured using the FM-7 microhardness tester.

3. Results and discussion

3.1. Structure

Fig. 1 shows the x-ray diffraction patterns for as- quenched melt- spun Sn-Zn alloys. It is found that the structure of all alloys consists of eutectic mixture of Sn and Zn solid solutions. The Zn phase precipitates in all alloys as indicated by Zn peaks as shown in Fig. 1. Both the number and the intensity of Zn peaks increases with increasing Zn concentration, which indicates more precipitation of Zn phase in the Sn matrix.

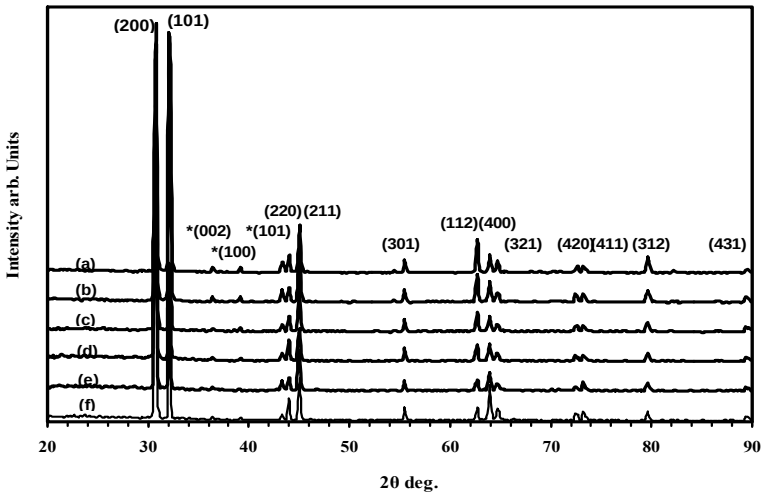

*Fig. 1. X-ray diffraction pattern for as quenched melt spun (a)Sn-6Zn, (b)Sn-7Zn, (c)Sn-8Zn, (d)Sn-9Zn and (e)Sn-10Zn (f) Sn-11Zn alloys. All peaks are for β-Sn and the peaks for Zn are indicated by *.*

Fig. 2.a and Fig.2.b show the variation of lattice parameters ***a***, ***c*** and the axial ratio ***c/a*** of the β- Sn matrix with valence electron concentration VEC. Both ***a*** and ***c*** decreases by increasing VEC to a minimum value and then increase by increasing VEC. The resulting axial ratio ***c/a*** is

shown in Fig. 2.c. ***c/a*** has a maximum value (0.5456) at VEC of 3.6643 corresponding to 8wt.% Zn, this means extension of the unit cell along c-axis and minimum value (0.5452) at VEC of 3.7595 corresponding to 7wt.% Zn which means the contraction of the unit cell along c-axis.

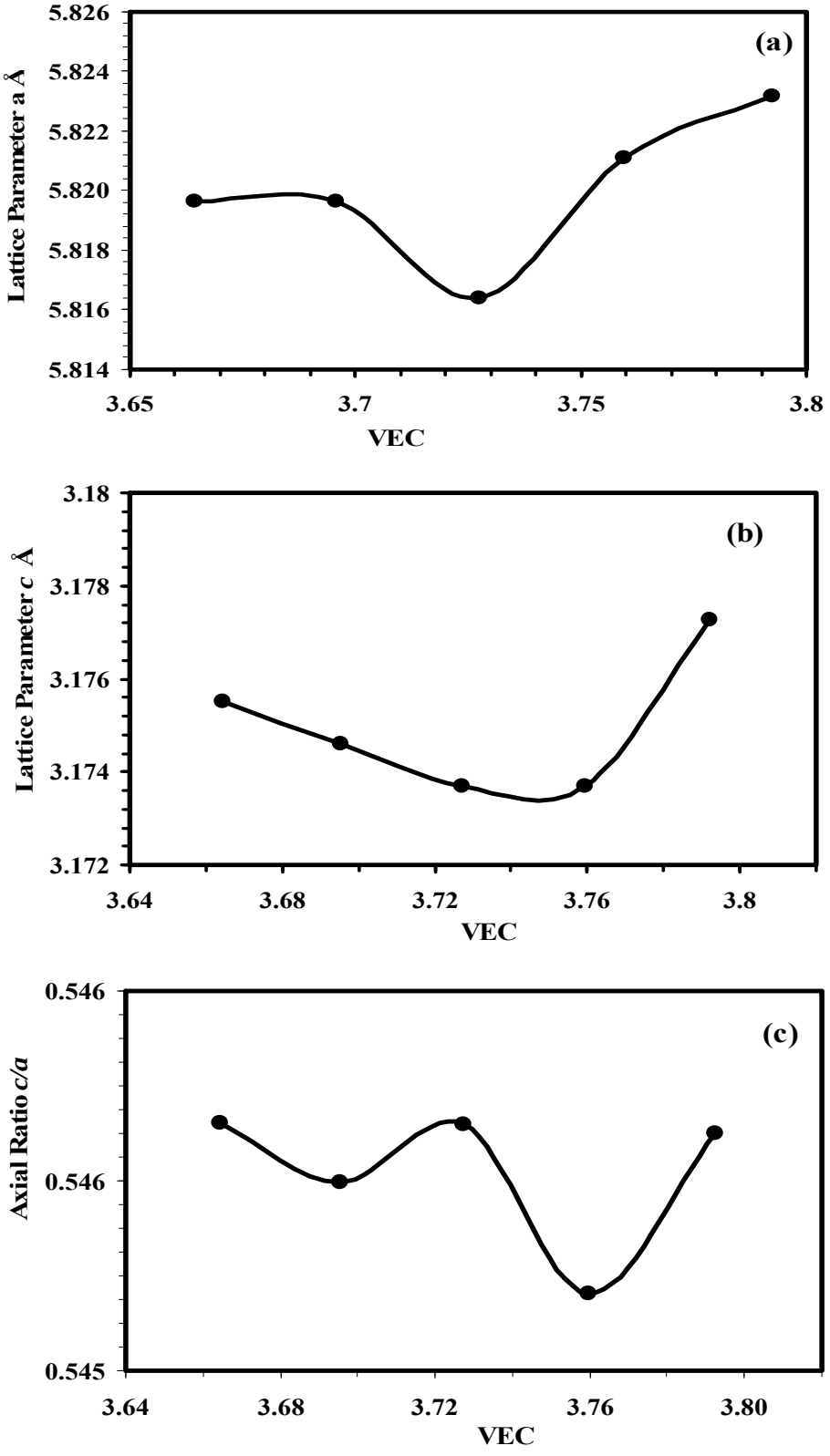

Fig. 2. The variations of lattice parameters (a) a, (b) c and (c) the axial ratio c/a.

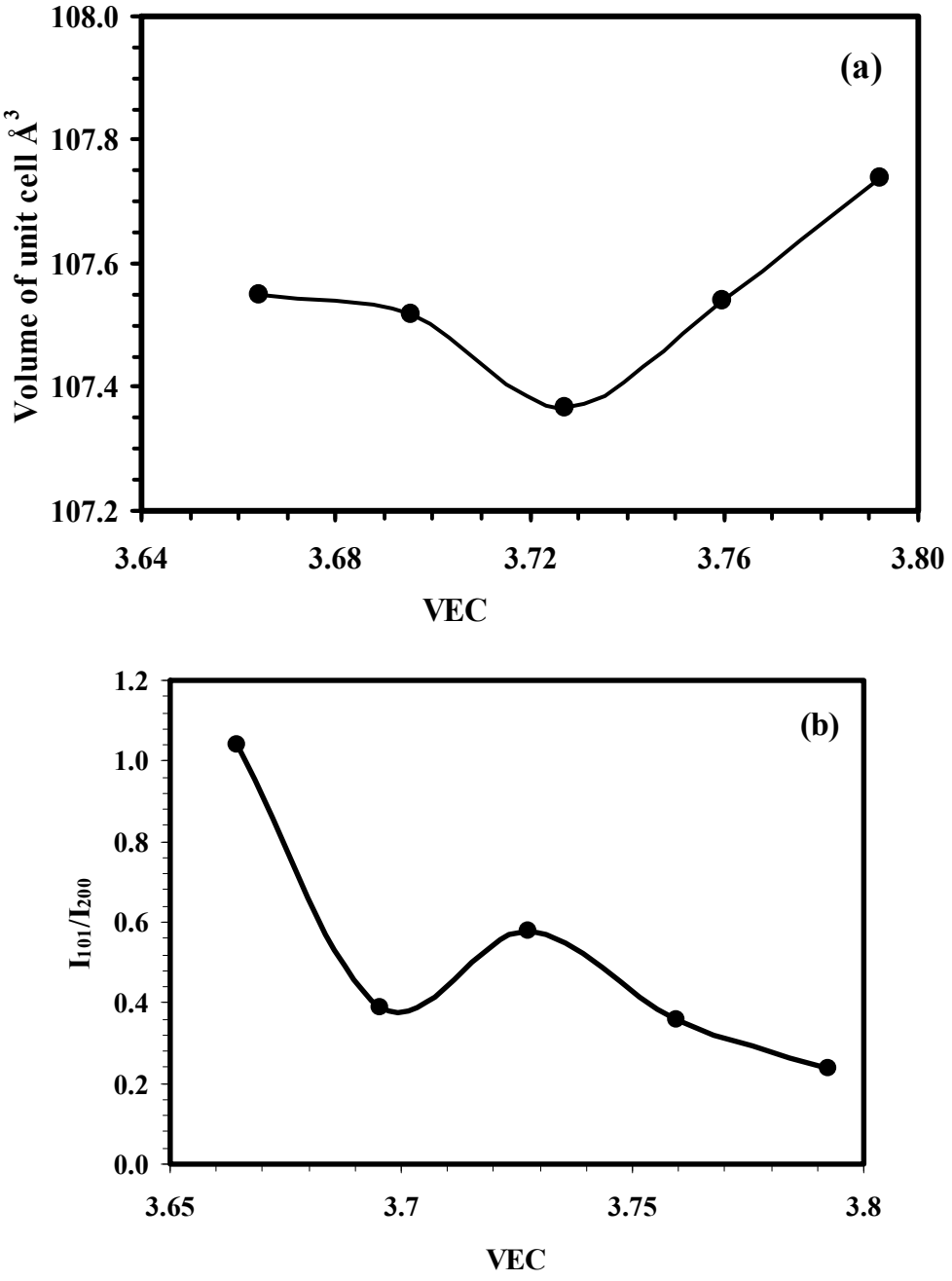

Fig. 3. The variation of (a) volume of unit cell and (b) intensity ratio from (101) and (200) planes with VEC.

Fig. 3.a shows the variation of volume of unit cell *v* with VEC. It is found that the volume of unit cell decreases by increasing VEC to a minimum value 107.368 at 3.727 corresponding to 8wt.% Zn and then increases to maximum value 107.74 at 3.792. (see also Table.1). Fig. 3.b shows the variation of the intensity ratio from (101) to (200) planes I_{101}/I_{200} of β-Sn matrix with VEC. It is found that the ratio decreases by increasing VEC. The value of I_{101}/I_{200} for pure Sn rapidly solidified was found to be 1.1 [10]. The addition of 6 wt.% Zn decreases this value to 0.237. This may be due to that the Zn atoms takes positions in (200) plane in the Sn lattice.

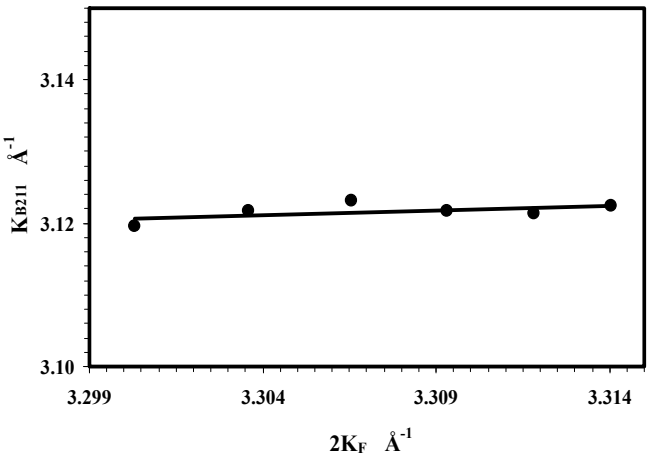

Fig. 4. The relationship between the diameter of the Brillouin zone K_B and the diameter of the Fermi sphere $2k_F$.

The relationship between the diameter of the Brillouin zone K_B and the diameter of the Fermi sphere $2k_F$ is shown in Fig. 4. A linear correlation is found between K_B and $2k_F$. As $2k_F$ increases, K_B increases in agreement of the condition of stability (see also Table. 1). The value of K_B is calculated for (211) planes. This is a direct evidence on the interaction between Fermi sphere and Brillouin zone and verification of Hume-Rothery condition of phase stability.

Table. 1:The Fermi parameters and the diameter of the Brillouin zone.

wt.% Zn in Sn	at.% Zn in Sn	VEC	n $\times 10^{23}$ (cm^{-3})	v (Å^3)	K_{B211} (Å^{-1})	$2k_F$ (Å^{-1})	E_F (eV)	$V_F \times 10^4$ (ms^{-1})
6	10.3829	3.79233	1.5176	107.7397	3.1196	3.3003	0.6473	1.9092
7	12.0199	3.75959	1.5221	107.5408	3.1217	3.30358	0.6485	1.9111
8	13.632	3.72735	1.5262	107.3679	3.1232	3.30657	0.6497	1.9129
9	15.2195	3.6956	1.5300	107.5188	3.1218	3.30931	0.6508	1.9144
10	16.7831	3.66432	1.5335	107.5492	3.1214	3.3118	0.6518	1.9159
11	18.3233	3.63352	1.5366	107.4611	3.1223	3.31406	0.6527	1.9172

From Table. 1 it is clear that as the Zn concentration increases VEC decreases since the valency of Zn is +2. All of the Fermi parameters decreases by increasing VEC and vice versa. The decrease in $\boldsymbol{v}$ with increasing VEC means that the volume of the first Brillouin zone increases by increasing VEC since they are inversely proportional to each other. This is also indicated by the increase in K_B with increasing VEC. Therefore by increasing VEC the diameter of Fermi sphere increases which leads to the increase of the diameter of Brillouin zone and which in turns due the decrease in the volume of the unit cell.

3.2 Thermal analysis

The DTA curves obtained for as- quenched melt- spun Sn-xZn alloys (x= 6, 7, 8, 9, 10, and 11 wt.%) are shown in Fig. 5. No phase transition before melting is observed. The variation of the enthalpy ΔH of fusion with valence electron concentration VEC is shown in Fig. 6.a. ΔH increases by increasing VEC to a maximum value 69.2×10^3 Jkg^{-1} at VEC of 3.727 and then ΔH decreases with VEC to a minimum value 45.68×10^3 Jkg^{-1} at VEC of 3.6956. The solidus T_s and liquidus T_l temperatures are shown in Fig. 6.b. It is evident that the Sn-10Zn alloy is the eutectic alloy because it has the lowest melting point. Also the eutectic reaction is found to occur at about 471 K.

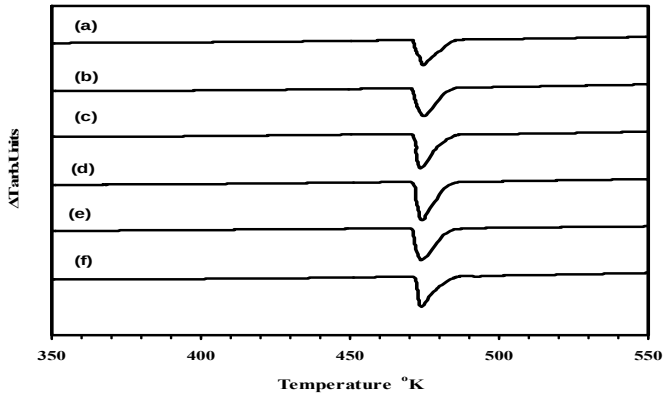

Fig. 5. Differential thermal analysis for as quenched melt spun (a)Sn-6Zn, (b)Sn-7Zn, (c)Sn-8Zn, (d)Sn-9Zn, (e)Sn-10Zn and (f)Sn-11Zn alloys.

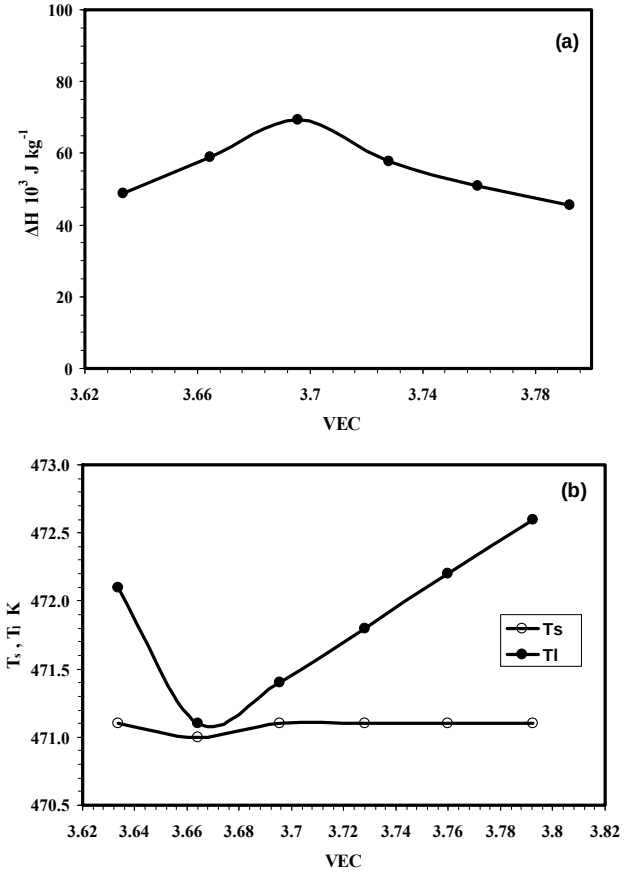

Fig. 6. The variation of (a) enthalpy of fusion, (b) solidus and liquidus temperatures with VEC.

3.3 Electrical properties

The temperature dependence of the electrical resistivity (ρ) of as-quenched melt-spun alloys is shown in Fig. 7.a. The resistivity increases linearly with temperature and there is no phase transition before melting in agreement with DTA results. Fig.7.b shows the variation of the resistivity at room temperature with valence electron concentration (VEC). The resistivity increase by increasing VEC up to maximum value 27.6×10^{-8} ohm.m at 3.727 corresponding to 8wt.% Zn and then decreases to minimum value 17.25×10^{-8} ohm.m at 3.82 corresponding to 5wt.% Zn. The decrease of can be explained in terms of VEC as the following; since the resistivity is given by $\rho = \frac{mv_f}{ne^2l}$ where m is the effective mass of the electron, v_f is Fermi velocity, n is the number of

electrons per unit volume, e the electron charge and l is the mean free path. From Table. 1 it is found that v_f decreases by increasing VEC, therefore the resistivity will decrease with VEC. The change in trend at VEC of 3.727 (corresponding to 8 wt.%) may be due to the inflection in both ***c/a*** and ***v*** which occurs at this composition.

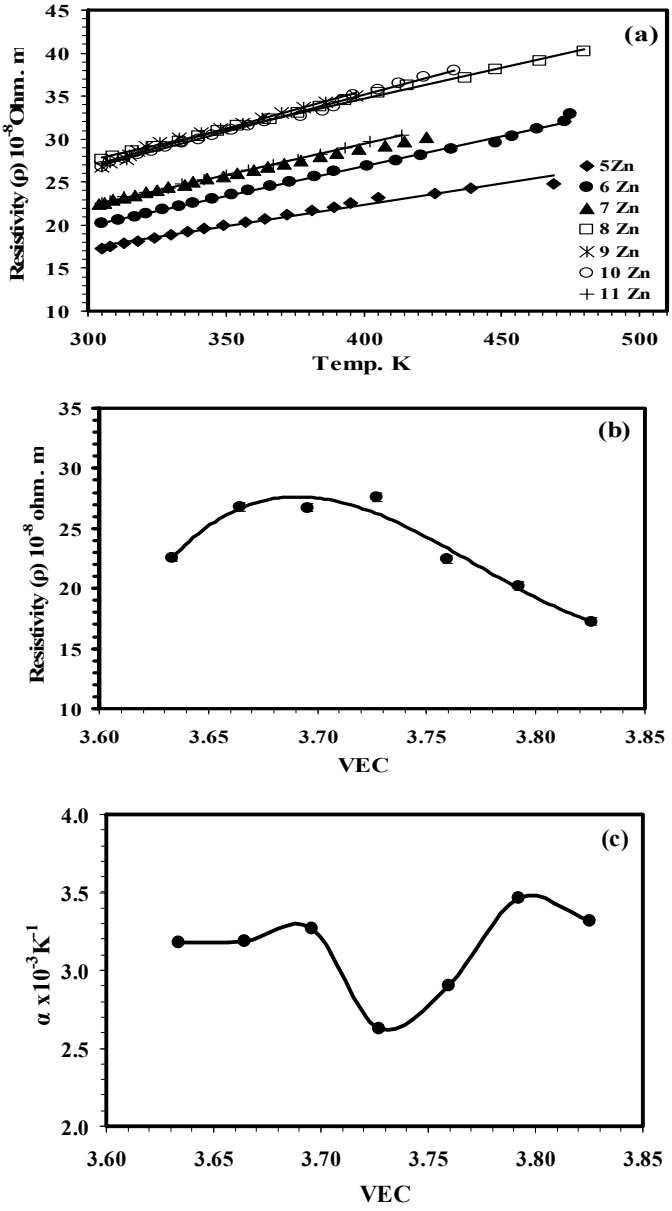

Fig. 7. (a) The temperature dependence of resistivity (b) The varaition of resistivity at room temperature and (c) temperature coefficient of resistivity with VEC.

Fig. 7.c shows the variation of temperature coefficient of resistivity α with VEC. It is found that α decreases with increasing VEC to minimum value 2.63 x10^{-3} K^{-1} at VEC 3.727 corresponding to 8 wt.% Zn and then increases by increasing VEC. The minimum value of α corresponding to the maximum value of ρ. Also a change in trend is found at 8 wt.% Zn which occurs also for ***c/a*** and ***v*** at this composition. It is well known that the relaxation time is inversely proportional to the temperature which leads to the linear dependence of the resistivity with temperature. Also the temperature coefficient of resistivity is inversely proportional to relaxation time. The relaxation

time is given by; $\tau = \frac{l}{v_f}$ Therefore as the relaxation time increases by increasing v_f this causes α to decrease with VEC since v_f decreases by increasing VEC as indicated in Table. 1.

3.4 Mechanical properties

Fig. 8.a shows the variation of Young's modulus (E) with valance electron concentration VEC. It is evident that E decreases by increasing VEC to a minimum value 42.11 GPa at 3.7272 corresponding to 8 wt.% Zn and then increases by increasing VEC. Also there is inflection in the trend observed at 8 wt.% which is also observed for ρ and α corresponding to the observed inflection for ***c/a*** and ***v***. E can be explained in terms of ***c/a*** since [4] observed a connection between E and ***c/a***. Fig. 8.b shows the variation of Young's modulus (E) with ***c/a***. E increases with increasing ***c/a*** up to certain critical value about 0.54562 after which E begin to decreases. The increase in ***c/a*** ratio means the stretching of the unit cell along the ***c***-axis, this modification in the shape of unit cell of Sn matrix may results in an increase in the bond strength which results in an increase in Young's modulus.

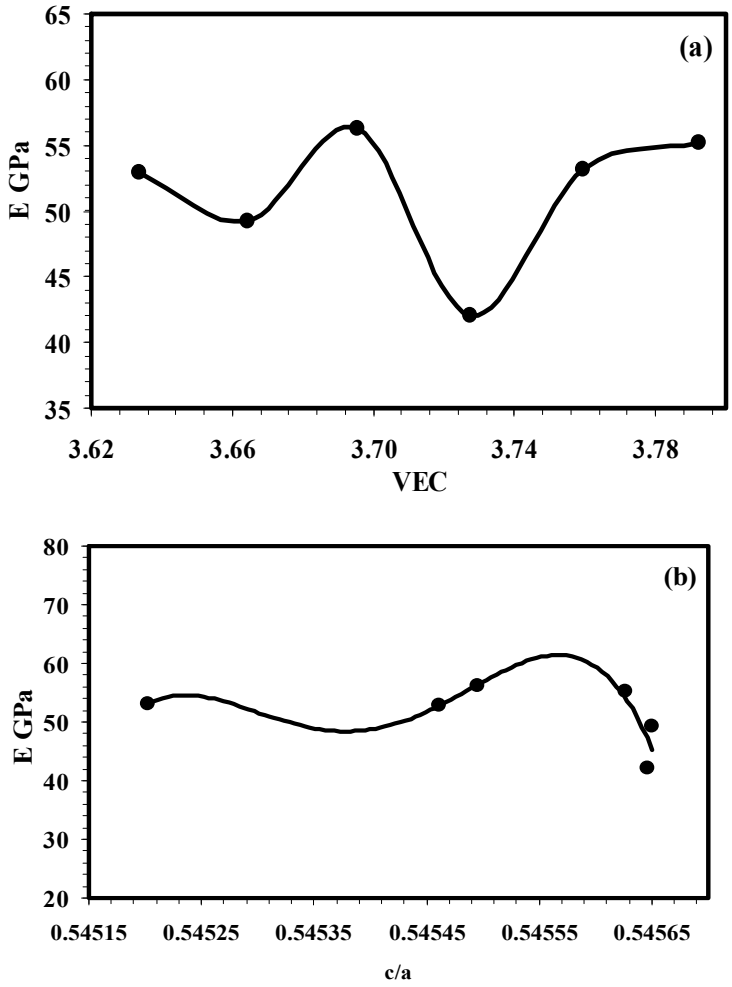

Fig. 8. Variation of Young's modulus with axial ratio (a) and VEC (b).

Fig. 9.a shows the variation of internal friction Q^{-1} with valence electron concentration VEC. The maximum value of Q^{-1} (43.54×10^{-2}) is observed at 3.7595 corresponding to 7 wt.% Zn and the minimum value (18.69×10^{-2}) is observed at 3.727 corresponding to 8 wt.% Zn. There are several mechanisms by which internal friction results such as the thermoelastic effect, the motion of interstitial and substitutional atoms, the intercrystalline thermal current and the motion of

dislocations. Which of these mechanisms is operative depends on the frequency. In the frequency range from 0.1 to 20 Hz used in the present work the mechanism inherent here is the motion of interstitial atoms. The movement of Zn atoms in the Sn lattice is restricted by the shape of the Sn unit cell this is clear if we notice the following. The maximum value of Q^{-1} is corresponding to the minimum value of ***c/a*** at VEC of 3.759 (7wt.% Zn). And the minimum value of Q^{-1} is corresponding to the maximum value of ***c/a*** at 3.727 (8wt.% Zn).

Fig. 9.b shows the variation of Vickers microhardness number HV with VEC. It is found that HV decreases with increasing VEC from 243 MPa to a 141 MPa. This means that HV increases by increasing Zn concentration. The increase in hardness due to the addition of Zn is attributed to two reasons. The first is solution hardening i.e. the substitutional Zn atoms cause local elastic strains in the Sn crystals. These local strains hinder the motion of dislocations and hence increase the hardness. The second reason is dispersion hardening i.e. the presence of a dispersion of small particles of Zn also hinder the motion of dislocations so increases the hardness.

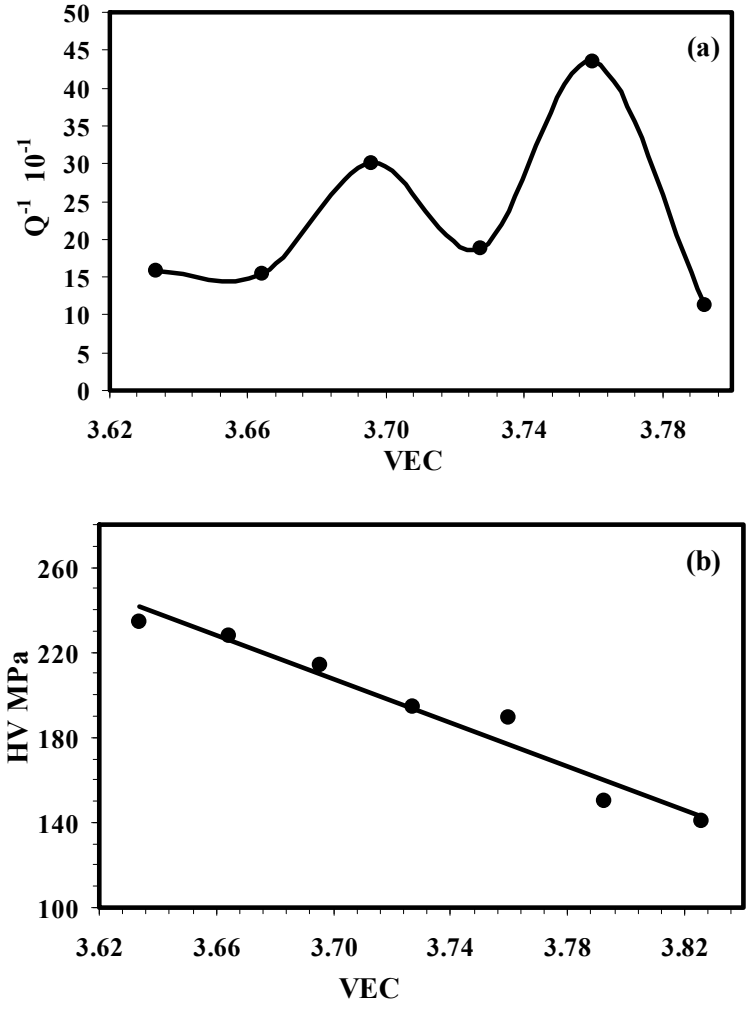

Fig. 9. Variation of internal friction (Q^{-1}) (a) and Vickers microhardness number (HV) (b) with VEC.

4.Conclusions

In this study the Hume-Rothery condition of phase stability has been verified. By increasing valence electron concentration VEC the diameter of Fermi sphere $2k_F$ increases which leads to the increase in the diameter of Brillouin zone. The electrical resistivity decreases by increasing VEC due to the decrease of the Fermi velocity with increasing VEC. Also it has been confirmed that the correlation between Young's modulus and the axial ratio ***c/a*** of β-Sn unit cell,

however there is critical value of ***c/a*** about 0.54562 beyond which E decreases. It is found also that the volume and shape of the unit cell affect both electrical and mechanical properties. In conclusion, valence electron concentration is the most important factor affecting the structure and properties changes of Sn-Zn alloys.

References

[1] W. Hume-Rothery, J. Inst. Met. **35**, 295 (1926).
[2] G. V. Raynor and J. A. Lee, Acta Met. **2**, 616 (1954).
[3] R. H. Kane, B. C. Giessen, and N. J. Grant, New metastable phases in binary tin alloy systems, Acta Met. 14 (1966) 605.
[4] Tarek El-Ashram, J. of Mater. Sci: Mater. in Electronics 16 (2005) 501-505.
[5] K. Schubert, U. Roseler, W. Mahler, E. Doerre, W. Schuett, Z. Metallk. **45**, 643 (1954).
[6] A.-P. Tsai, J. of Non-Crystalline Solids, **334&335**, 317 (2004).
[7] Mustafa Kamal, Abu Bakr El-Bediwi and Tarek El-Ashram, J. of Mater. Sci: Mater in Electronics **15**, 211 (2004).
[8] Yu. A. Geller, A. G. Rakhshtadt, Science of Materials, (Mir Publishers, Moscow, 1977) p. 138.
[9] E. Schreiber, O. L. Anderson and N. Soga, "Elastic Constants, and their Measurements" (McGraw Hill book Company, 1973) p. 82.
[10] Tarek El-Ashram, Radiation Effects and Defects in Solids, **161**, 193 (2006).

Universal Behaviour of Binary Amorphous Alloys Containing Noble Mentals and Simple Metals and Their Description in the Frame of a New Hume-Rothery Phase. Some Fundamental Aspects of Solidification in a Supercooled Melt. Interface Morphology During Rapid Solidification. Cellular Solidification in Ni Based Melt Spun Alloys. Relationships Between Microstructure and Processing in Melt Spun Al-Fe Alloys.Â Second Phase Coarsening in Rapidly Solidified Ti-5sn-4.5 La System. The Production of Ultrafine Dispersions of Rare Earth Oxides in Ti Alloys Using Rapid Solidification. Structure, Mechanical and Electrical Properties of Rapidly Quenched Aluminium-Silicon Alloys.